1-1-2011

Depositional Ice Nucleation onto Hydrated NaCl Particles: a New Mechanism for Ice Formation in the Troposphere

M. E. Wise
University of Colorado, Boulder, mawise@cu-portland.edu

K. J. Baustian
University of Colorado, Boulder

T. Koop
Bielefeld University

M. A. Freedman
The Pennsylvania State University

E. J. Jensen
NASA Ames Research Center

See next page for additional authors

Atmos. Chem. Phys. Discuss., 11, 23139–23167, 2011
www.atmos-chem-phys-discuss.net/11/23139/2011/
doi:10.5194/acpd-11-23139-2011

Atmospheric Chemistry and Physics Discussions

Depositional ice nucleation onto hydrated NaCl particles: a new mechanism for ice formation in the troposphere

M. E. Wise[1,2], **K. J. Baustian**[2,3], **T. Koop**[4], **M. A. Freedman**[5], **E. J. Jensen**[6], **and M. A. Tolbert**[1,2]

[1]Department of Chemistry & Biochemistry, University of Colorado, Boulder, CO 80309, USA
[2]Cooperative Institute for Research in Environmental Sciences, University of Colorado, Boulder, CO 80309, USA
[3]Department of Atmospheric and Oceanic Science, University of Colorado, Boulder, CO 80309, USA
[4]Faculty of Chemistry, Bielefeld University, 33615 Bielefeld, Germany
[5]Department of Chemistry, The Pennsylvania State University, University Park, PA 16802, USA
[6]NASA Ames Research Center, Moffett Field, CA, USA

Received: 27 July 2011 – Accepted: 29 July 2011 – Published: 17 August 2011

Correspondence to: M. A. Tolbert (tolbert@colorado.edu)

Published by Copernicus Publications on behalf of the European Geosciences Union.

Abstract

Sea-salt aerosol particles (SSA) are ubiquitous in the marine boundary layer and over coastal areas. Therefore SSA have ability to directly and indirectly affect the Earth's radiation balance. The influence SSA have on climate is related to their water uptake and ice nucleation characteristics. In this study, optical microscopy coupled with Raman spectroscopy was used to detect the formation of an NaCl hydrate that could form under atmospheric conditions. $NaCl_{(s)}$ particles deliquesced at the well established value of 75.7 ± 2.5 % RH. $NaCl_{(aq)}$ particles effloresced to a mixture of hydrated and non-hydrated particles at temperatures between 236 and 252 K. The aqueous particles effloresced into the non-hydrated form at temperatures warmer than 252 K. At temperatures colder than 236 K all particles effloresced into the hydrated form. The deliquescence relative humidities (DRH) of hydrated $NaCl_{(s)}$ particles ranged from 76.6 to 93.2 % RH. Based on the measured DRH and efflorescence relative humidities (ERH), we estimate crystalline NaCl particles could be in the hydrated form 40–80 % of the time in the troposphere. Additionally, the ice nucleating abilities of $NaCl_{(s)}$ and hydrated $NaCl_{(s)}$ were determined at temperatures ranging from 221 to 238 K. $NaCl_{(s)}$ particles depositionally nucleated ice at an average S_{ice} value of 1.11 ± 0.07. Hydrated $NaCl_{(s)}$ particles depositionally nucleated ice at an average S_{ice} value of 1.02 ± 0.04. When a mixture of hydrated and anhydrous $NaCl_{(s)}$ particles was present in the same sample, ice preferentially nucleated on the hydrated particles 100 % of the time. While both types of particles are efficient ice nuclei, hydrated $NaCl_{(s)}$ particles are better ice nuclei than $NaCl_{(s)}$ particles.

1 Introduction

It is known that sea-salt aerosol particles (SSA) are ubiquitous in the marine boundary layer and over coastal areas. These particles are injected into the atmosphere due to wind and wave action over oceans. It is estimated that 1×10^{12} to 1×0^{13} kg of

ACPD
11, 23139–23167, 2011

SSA enters the atmosphere per year (Blanchard, 1985). Therefore it is appropriate that studies have been carried out to estimate the radiative effects of SSA particles. Haywood et al. (1999) estimated the direct radiative effect of SSA particles to be −1.5 to $-5\,W\,m^{-2}$. Vinoj and Satheesh (2003) estimated the indirect radiative effect arising from the CCN activity of SSA over the Indian Ocean to be $-7 \pm 4\,W\,m^{-2}$.

SSA are made up of many different chemical compounds. The ionic composition of dry, freshly emitted SSA can be inferred from the composition of natural seawater. Natural seawater contains 55.40 % (w/w) Cl^-, 30.61 % Na^+, 7.68 % SO_4^{2-} and 3.69 % Mg^{2+} (Pilson, 1998). It is also known that natural SSA contains on the order of 10 % (w/w) organic compounds (Middlebrook et al., 1998). Once emitted into the atmosphere, SSA composition can change due to heterogeneous reactions in the atmosphere. For example, nitric acid can react with SSA to form gaseous hydrogen chloride and (depending on atmospheric conditions) aqueous or solid sodium nitrate (i.e., De Haan and Finlayson-Pitts, 1997).

Although natural SSA are chemically complex (which can affect water uptake properties) NaCl has been widely used as a proxy for SSA. Therefore, several studies have been conducted to determine the conditions under which NaCl particles take up water to form solution droplets (deliquescence) and lose water to reform crystalline NaCl particles (efflorescence). It is widely accepted that, at room temperature, pure NaCl particles deliquesce at approximately 75 % relative humidity (DRH) and effloresce at approximately 45 % relative humidity (ERH) (i.e., Cziczo and Abbatt, 2000; Koop et al., 2000; Tang et al., 1977; Wise et al., 2005). Additionally, using a flow-tube apparatus, Cziczo and Abbatt (2000) found that the DRH and ERH of NaCl particles did not change substantially when temperature was decreased from 298 to 253 K. Koop et al. (2000) extended the temperature range at which the DRH and ERH of NaCl particles were determined using differential scanning calorimetry (DSC) measurements and flow cell microscopy. In agreement with Cziczo and Abbatt (2000), Koop et al. (2000) found that the DRH of NaCl particles did not change substantially at temperatures as low as 239 K.

ACPD
11, 23139–23167, 2011

Because NaCl is a ubiquitous tropospheric particle, it is important to elucidate the behavior of NaCl particles at even lower temperatures found throughout the troposphere. According to the NaCl phase diagram (1965), at maximum NaCl solubility, a brine solution and the crystalline dihydrate form of NaCl ($NaCl{\bullet}2H_2O_{(s)}$) are stable from 273 K to the eutectic temperature of 252 K. At temperatures below 252 K, solid ice and $NaCl{\bullet}2\ H_2O_{(s)}$ (sodium chloride dihydrate) are stable. Cziczo and Abbatt (2000) did not find indications of $NaCl{\bullet}2H_2O_{(s)}$ formation (at conditions predicted by the bulk phase diagram) during their NaCl water uptake experiments. Similarly Koop et al. (2000) did not find indications of $NaCl{\bullet}2H_2O_{(s)}$ formation in their low temperature flow cell experiments because the DRH of the solid particles did not agree with the predicted DRH for $NaCl{\bullet}2H_2O_{(s)}$. However, Koop et al. (2000) did find indications of $NaCl{\bullet}2H_2O_{(s)}$ in their DSC experiments which was attributed to heterogeneous nucleation on available ice surfaces after ice formation.

Cziczo et al. (2004) performed an in-situ investigation of the chemical composition of anvil cirrus cloud residue near the Florida peninsula. They found that 26 % of the ice residue in the Florida area was sea salt. Cziczo et al. (2004) encountered cirrus clouds that appeared to incorporate both heterogeneous and homogeneous ice nucleation simultaneously. They inferred that sea salt likely nucleated ice via a homogeneous freezing mechanism and that insoluble particles (such as mineral dust) nucleated ice via a heterogeneous freezing mechanism. This inference was made due to the observation that sea salt particles dominated the larger size mode. However, it is possible that ice nucleated on hydrated $NaCl_{(s)}$ particles which would also be larger than anhydrous NaCl.

In the present study we re-examine NaCl deliquescence, efflorescence and ice nucleation at low temperatures. We use a combination of optical microscopy and Raman spectroscopy to probe the phase transitions and ice nucleating efficiency of sodium chloride particles under a range of tropospheric conditions. Specifically, this combination of techniques allows the visual and spectroscopic determination of the conditions at which micron-sized $NaCl_{(s)}$, $NaCl_{(aq)}$, and hydrated $NaCl_{(s)}$ particles are stable at

ACPD
11, 23139–23167, 2011

tropospheric temperature conditions. It also allows a comparison of the depositional ice nucleating ability of $NaCl_{(s)}$ and hydrated $NaCl_{(s)}$.

2 Experimental

A Nicolet Almega XR Dispersive Raman spectrometer outfitted with a modified Linkham THMS600 environmental cell, a Buck Research Instruments CR-1A chilled mirror hygrometer, and a Linkham automated temperature controller was used to study deliquescence, efflorescence and depositional ice nucleation using pure $NaCl_{(s)}$ and hydrated $NaCl_{(s)}$ particles. The Raman spectrometer was equipped with an Olympus BX51 research-grade optical microscope which had the capability to magnify particles 10×, 20×, 50× and 100×. The experimental setup and procedure is similar to that used in Baustian et al. (2010) and Wise et al. (2010). A brief description of the experiment is given here with detail given when the current experiment differs from that of Baustian et al. (2010) and Wise et al. (2010).

NaCl particles were generated by feeding a 10 wt % NaCl solution at 2 ml min^{-1} into an atomizer (TSI 3076) using a Harvard apparatus syringe pump. Pre-purified nitrogen gas at a flow rate of 3000 ccm was used to operate the atomizer. The particles exiting the atomizer were then impacted onto a hydrophobic quartz disc for analysis. The diameters of the particles studied ranged from approximately 1 to 10 µm with typical values close to 5 µm.

2.1 Deliquescence and efflorescence of $NaCl_{(s)}$ and hydrated $NaCl_{(s)}$ particles

To begin a water uptake experiment, the silanized quartz disc containing $NaCl_{(s)}$ particles was placed inside the environmental cell at room temperature. The cell was sealed and water vapor was purged from the cell using a flow of ultra-high purity nitrogen. Once the frost point in the environmental cell reached approximately 213 K, the temperature of the particles was lowered to between 233 and 258 K using a combination

ACPD
11, 23139–23167, 2011

of liquid nitrogen cooling and resistive heating. After the temperature of the particles equilibrated, water vapor was introduced into the cell until deliquescence was visually observed at 50× magnification. Raman spectra of the particles were then taken for verification.

After deliquescence, water vapor was removed from the cell until efflorescence of all particles was observed. As with the deliquescence phase transition, efflorescence was monitored both visually and spectroscopically. Depending on particle temperature, either $NaCl_{(s)}$, hydrated $NaCl_{(s)}$ or a mixture of the two solid forms nucleated when the particles effloresced. If hydrated $NaCl_{(s)}$ formation was observed, the particles were subjected to a second RH cycle to determine the DRH and ERH of the hydrated particles. After each particle effloresced following the second RH cycle, Raman spectra of 50 different particles were collected to determine the percentage of solid particles that were anhydrous $NaCl_{(s)}$. In order to eliminate operator bias, 50 random particles were studied. Specifically, the substrate was moved in a straight line and each particle that was illuminated by the Raman laser was studied.

2.2 Depositional ice nucleation on $NaCl_{(s)}$ and hydrated $NaCl_{(s)}$ particles

To begin a depositional ice nucleation experiment on $NaCl_{(s)}$ particles, a quartz disc containing $NaCl_{(s)}$ particles was placed inside the environmental cell at room temperature. The cell was sealed, water vapor purged and the temperature of the particles was lowered to between 221 and 238 K. Water vapor was introduced into the cell continuously until ice nucleation was visually observed (at 10× magnification) and S_{ice} was recorded. Ice was confirmed using Raman spectroscopy. After the confirmation of ice, the water vapor was shut off and the ice was sublimed. A Raman spectrum of the ice nuclei (IN) was taken.

Depositional ice nucleation on a sample containing both $NaCl_{(s)}$ and hydrated $NaCl_{(s)}$ particles was also studied. Hydrated $NaCl_{(s)}$ could not be made at room temperature. Therefore, the experiment was initiated by deliquescing $NaCl_{(s)}$ and then efflorescing the particles at approximately 239 K. This was accomplished using the

ACPD
11, 23139–23167, 2011

deliquescence/efflorescence procedure described above. A temperature of 239 K was chosen because it was experimentally determined that (after efflorescence) the majority of the particles were hydrated $NaCl_{(s)}$. However, some anhydrous $NaCl_{(s)}$ particles also formed. After the formation of the hydrated particles, the temperature of the particles was lowered to between 221 and 238 K at a rate of 2 K min^{-1}. As the temperature of the particles decreased from 239 K, it was important to maintain the RH in the environmental cell at values between 25 and 45 %. This RH range was chosen because at low RH values (6–25 %), the hydrated NaCl particles reverted to the anhydrous form and at high RH values (75 %) the anhydrous particles deliquesced. Furthermore, the cooling rate of 2 K min^{-1} was chosen so that an S_{ice} of greater than 1 was not attained before the desired temperature was reached. Once the solid particles reached the desired temperature, water vapor was introduced into the cell until ice nucleation was visually observed (at 10× magnification). Ice was confirmed using Raman spectroscopy. After the confirmation of ice, the water vapor was shut off and the ice was sublimed. A Raman spectrum of the IN was taken.

3 Results

Figure 1 presents images of NaCl particles (at 50× magnification) recorded from the optical microscope as RH was cycled from 0 to 76 % at 244 K. At 0.9 % RH, all of the particles on the quartz disc were $NaCl_{(s)}$. As RH was increased to 69.0 %, the morphology of the particles did not change and no water uptake was observed. At 69.0 % RH, the solid NaCl particles visually took up a small amount of water. The presence of water on particle "a" in Fig. 1 was confirmed using Raman spectroscopy. The spectrum is recorded in Fig. 2. Although subtle, the Raman signal due to water uptake is seen as a small increase in intensity over the broad range of 3000 to 3700 cm^{-1}. The DRH of $NaCl_{(s)}$ particles is known to be ~75 % RH at 244 K which is higher than the RH observed here for the onset of water uptake. However, the $NaCl_{(s)}$ particles at 69.0 % were not fully dissolved. At this point, if the water vapor in the environmental

ACPD
11, 23139–23167, 2011

cell were reduced, the particles would revert to their fully crystalline state. Slight water uptake prior to deliquescence was also observed on ammonium sulfate particles using Raman microscopy (Wise et al., 2010) and a variety of other soluble salt compounds using an environmental transmission electron microscope (Wise et al., 2008). Similar water uptake below the bulk DRH was also observed for other particles using H-TDMA and may be interpreted as water absorption into polycrystalline particles owing to capillary effects (Mikhailov et al., 2009). At 75.4 % RH, the $NaCl_{(s)}$ particles deliquesced. Deliquescence resulted in a notable increase in the Raman intensity between 3000 to 3700 cm^{-1} (Fig. 2b) and was visually confirmed by noting the RH at which the $NaCl_{(s)}$ core disappeared. The DRH of the $NaCl_{(s)}$ particles found in this experiment agrees well with the accepted value for $NaCl_{(s)}$.

After deliquescence, the RH in the environmental cell was decreased to 45.3 % RH and the particles gradually lost water resulting in decreasing size. At 45.3 % RH, one of the particles in the field of view effloresced (particle "c"). This particle did not effloresce into morphology consistent with that of $NaCl_{(s)}$. Particle "c" appeared round and bumpy whereas $NaCl_{(s)}$ particles appeared cubic. The Raman spectrum taken of particle "c" is included in Fig. 2. The spectrum has sharp Raman intensities at approximately 3530 cm^{-1} and 3410 cm^{-1}. The Raman spectrum of particle "c" is markedly different than that of $NaCl_{(s)}$ because $NaCl_{(s)}$ shows no features in this region. As the RH in the environmental cell decreased to 40.4 %, a cubic $NaCl_{(s)}$ particle formed (particle "d"). The Raman spectrum shown in Fig. 2 confirms that the particle is $NaCl_{(s)}$ due to the lack of peaks in the spectrum. When the RH decreased further to 35.9 % RH (Fig. 1), all the particles reverted to their solid form. In this particular experiment, the efflorescence of $NaCl_{(aq)}$ droplets occurred over a range of 35.9 to 45.3 % RH. The range of ERH values is not surprising given the stochastic nature of efflorescence and lies within the range of previously observed values (43–50 % RH; Martin, 2000).

From the water uptake experiment described above, it is apparent that two different forms of solid NaCl effloresced at 244 K. According to the bulk NaCl phase diagram (Linke, 1965), aqueous NaCl droplets are not stable at 244 K. Depending on the wt % of

ACPD
11, 23139–23167, 2011

NaCl, either a mixture of ice and $NaCl{\bullet}2H_2O_{(s)}$ or a mixture of $NaCl_{(s)}$ and $NaCl{\bullet}2H_2O_{(s)}$ is predicted to be present. Therefore, in the current experiment, the aqueous droplets that nucleated solid particles between 36 and 45 % RH were in a metastable state prior to efflorescence. This result is not surprising given the fact that micron sized liquid water particles do not homogeneously nucleate ice until a temperature of approximately 233 K (see review by Koop, 2004)

A question arises concerning the identity of the second form of solid NaCl. Ice is obviously not present in the particles because the signature of ice does not appear in the Raman spectrum. The next logical choice for the identity of the solid is $NaCl{\bullet}2H_2O$ due to its presence in the bulk NaCl phase diagram. Dubessy et al. (1982) used the Raman microprobe MOLE to collect the Raman spectrum of $NaCl{\bullet}2H_2O_{(s)}$ at 103 K. The Raman spectrum collected by Dubessy et al. (1982) had 8 sharp peaks. The positions of those peaks are highlighted with solid lines on a Raman spectrum of the non-cubic form of $NaCl_{(s)}$ (collected in this experiment at 244 K) in Fig. 3a. The Raman spectrum collected at 244 K did not have 8 distinct peaks; however, the peaks from the Dubessy et al. (1982) spectrum line up well with the peaks that are present. Perhaps the differences between the Dubessy et al. (1982) spectrum of $NaCl{\bullet}2H_2O_{(s)}$ and the spectrum collected here is not due to a difference in composition but to differences in the temperatures at which the spectra were collected (103 K versus 244 K). To check this, the temperature of the particles was lowered to the minimum temperature attainable in the environmental cell (163 K). The Raman spectrum of the non-cubic form of $NaCl_{(s)}$ collected at 163 K is shown in Fig. 3b. Two peaks at ~3209 cm^{-1} and 3089 cm^{-1} appeared in the Raman spectrum when the temperature was lowered to 163 K. These peaks match well with the peaks in the spectrum of $NaCl{\bullet}2H_2O_{(s)}$ collected by Dubessy et al. (1982) at 103 K. Therefore, the non-spherical, solid particles present in Fig. 1 definitively contain waters of hydration and are possibly $NaCl{\bullet}2H_2O_{(s)}$.

Assuming that particle size does not affect thermodynamics, the DRH of $NaCl_{(s)}$ should correspond to its solubility line in the bulk phase diagram. This is expected because particle size has been shown to affect ERH and DRH only below 100 nm in

ACPD
11, 23139–23167, 2011

diameter (Biskos et al., 2006). Since the particles used in this experiment are significantly greater than 100 nm, the DRH of $NaCl_{(s)}$ and $NaCl{\bullet}2H_2O_{(s)}$ should be predicted well using the bulk phase diagram. In order to test this prediction, a second water uptake experiment was conducted on a sample of mixed $NaCl_{(s)}$ and hydrated $NaCl_{(s)}$ particles. The results of a typical water uptake experiment with a sample of mixed phase particles are shown in Fig. 4. This water uptake experiment was a continuation of the water uptake experiment performed at 244 K shown in Fig. 1. Therefore all the particles are the same.

At RH values less than 76.3 % all of the particles were solid but some were hydrated and some were anhydrous. As the RH in the environmental cell was increased to 76.3 %, the $NaCl_{(s)}$ particles deliquesced (see circled particle) and the hydrated $NaCl_{(s)}$ (see particle in the square) particles remained in the solid phase. A DRH of 76.3 % for $NaCl_{(s)}$ particles is consistent with the theoretical DRH for $NaCl_{(s)}$ particles at this temperature. When the RH was increased to 89.6 % RH, the hydrated $NaCl_{(s)}$ particles deliquesced. Once all the particles deliquesced, water vapor was removed from the environmental cell until all the particles effloresced. All particles effloresced by 32.5 % RH. Interestingly, some of the particles effloresced into a phase that they did not originally start in. For example, the particle highlighted with the box started the RH cycle as a hydrated particle and finished the RH cycle as an anhydrous particle. The waters of hydration in the crystal lattice of the hydrated $NaCl_{(s)}$ particles were removed when the RH in the environmental cell was dropped to 19.8 %. This transformation was accompanied by the cracking of the particle and the disappearance of all peaks in the Raman spectrum. This phenomenon is evident in the last panel of Fig. 4.

Figure 5 shows the NaCl phase diagram adapted from Koop et al. (2000) in temperature/RH space rather than temperature/wt% space. Koop et al. (2000) described the construction of the phase diagram; therefore, only descriptions of the symbols are given here. The thick solid vertical line represents the accepted DRH values for $NaCl_{(s)}$ particles and the thick dotted vertical line represents the accepted ERH values for $NaCl_{(aq)}$ particles. These values are based on experimental measurements between 278 and

ACPD
11, 23139–23167, 2011

308 K. The thin lines extending from the accepted DRH and ERH lines are extrapolations to lower temperatures. The open diamonds and crosses represent the DRH and ERH of the NaCl particles studied here at temperatures between 233 and 256 K. The DRH of $NaCl_{(s)}$ and the ERH of $NaCl_{(aq)}$ particles measured here agree well with the extrapolated values of DRH and ERH. Furthermore, the measurements agree with the DRH (filled circles) and ERH (filled squares) observed by Koop et al. (2000) using a flow cell apparatus. Using a flow tube apparatus at temperatures between 253 and 283 K, Cziczo et al. (2000) also studied the water uptake properties of NaCl particles. The DRH and ERH measurements made by Cziczo et al. (2000) also agree with the measurements made here.

It was previously shown (Fig. 1) that at 244 K a mixture of $NaCl_{(s)}$ and hydrated $NaCl_{(s)}$ particles form upon efflorescence of solution droplets. It was found that at temperatures warmer than 252 K, no hydrated $NaCl_{(s)}$ particles formed upon efflorescence. However, at temperatures between 236 and 252 K, a mixture of hydrated and anhydrous particles effloresced. The temperature region in which both hydrated and anhydrous particles nucleated is denoted with light gray shading in Fig. 5. Efflorescence experiments performed at temperatures colder than 236 K produced only hydrated $NaCl_{(s)}$. This temperature region is denoted with darker gray shading in Fig. 5. Because a mixture of hydrated and anhydrous particles formed between 236 and 252 K, efflorescence experiments were conducted to find the relationship between particle temperature and the percentage of particles in the anhydrous form. The results of these experiments are shown in Fig. 6. Between 239 and 249 K, there is a linear relationship between the temperature of the particles at efflorescence and the percentage of anhydrous $NaCl_{(s)}$ particles formed. Although hydrated particles form between 236 and 239 K, the linear relationship between temperature and the percentage of anhydrous $NaCl_{(s)}$ particles formed breaks down. Similarly, between 249 and 252 K, the linear relationship is not valid. Therefore, between 239 and 249 K, the percentage of anhydrous $NaCl_{(s)}$ particles can be predicted if particle temperature is known.

ACPD
11, 23139–23167, 2011

Water uptake experiments were performed on hydrated $NaCl_{(s)}$ particles at temperatures between 235 and 247 K to determine their DRH. The results of these experiments are denoted with green crossed circles in Fig. 5. The DRH of the hydrated particles found in this study do not agree with the theoretical DRH of $NaCl{\bullet}2H_2O_{(s)}$ (thick dashed line). This result is at odds with spectral evidence showing that the hydrated particles are most likely $NaCl{\bullet}2H_2O_{(s)}$. Additional water uptake experiments were performed on samples containing only hydrated particles. The DRH values determined in these experiments agreed well with the DRH values found in the mixed particle experiments. The question then remains as to why the hydrated particles do not deliquesce at the RH predicted for $NaCl{\bullet}2H_2O_{(s)}$.

We cannot exclude the formation of another type of hydrate that has not been observed previously in the literature. While this could explain why the observed DRH values are different from those predicted for the dihydrate from bulk data, it appears to be inconsistent with the spectroscopic data. However, whether the hydrate observed in our experiments is identical to the dihydrate observed in bulk experiments, or is a metastable form of the dihydrate, or is yet another higher hydrate does not affect any of the conclusions drawn below.

Although the identity of the non-cubic, hydrated form of the $NaCl_{(s)}$ particles is not fully understood, their ice nucleating ability can be probed and compared to $NaCl_{(s)}$. Figure 7 shows the results of a typical ice nucleating experiment on a sample containing both anhydrous and hydrated $NaCl_{(s)}$ particles. The mixed sample was created by deliquescing $NaCl_{(s)}$ particles and then efflorescing them at ~239 K. After efflorescence, particle temperature was decreased to 224 K while the RH in the environmental cell was maintained at RH values between 25 and 45 %. In this particular experiment, when the RH in the environmental cell was increased to ~63 % (at 224 K), ice began to nucleate on top of one of the hydrated particles. In order to confirm that ice was nucleating on a hydrated particle, Raman spectra were taken of the ice and the ice nuclei. The Raman spectrum (spectrum "a" in Fig. 7) had peaks indicitive of a hydrated $NaCl_{(s)}$ particle and ice. After the ice was sublimed from the sample, a Raman spectrum was

ACPD
11, 23139–23167, 2011

collected (spectrum "b" in Fig. 7) of the ice nuclei. This spectrum again confirmed that the ice nucleus was a hydrated particle. In this particular experiment, ice formed on the hydrated particles at an S_{ice} of 1.01.

Several ice nucleation experiments were performed on mixed anhydrous and hydrated $NaCl_{(s)}$ samples at various temperatures. The results of these experiments are plotted in Fig. 8 in S_{ice}/temperature space. A temperature range of 221 to 238 K was chosen in order to compare the ice nucleating ability of hydrated $NaCl_{(s)}$ with that of ammonium sulfate (Baustian et al., 2010). Over the temperature range studied, it can be seen that the hydrated $NaCl_{(s)}$ particles nucleate ice at S_{ice} values between 0.97 and 1.11 (open circles in Fig. 8). Additionally, there does not appear to be a temperature dependence of the ice nucleating ability of hydrated $NaCl_{(s)}$ particles. The average S_{ice} value for the 21 experiments is 1.02 ± 0.04. The saturation ratio needed for hydrated $NaCl_{(s)}$ particles to nucleate ice is lower than that of ammonium sulfate particles ($S_{ice} \sim 1.1$, Baustian et al., 2010).

Using the mixed samples, it was observed that the ice nucleated preferentially on the hydrated $NaCl_{(s)}$ particles over the anhydrous particles. In every case, the hydrated $NaCl_{(s)}$ particles nucleated ice before the anhydrous $NaCl_{(s)}$ particles. In order to confirm this observation, ice nucleation experiments were performed on samples containing only anhydrous $NaCl_{(s)}$ particles (filled squares in Fig. 8). Over the same temperature range, anhydrous $NaCl_{(s)}$ particles nucleated ice at S_{ice} values between 1.02 and 1.21. The average S_{ice} value for the 9 experiments performed on anhydrous $NaCl_{(s)}$ particles is 1.11 ± 0.07.

In the above experiments, hydrated $NaCl_{(s)}$ particles were sometimes observed to undergo deliquescence and sometimes depositional ice nucleation occurred. To examine the two processes, the depositional ice nucleation and deliquescence data for the hydrated $NaCl_{(s)}$ particles are plotted in RH versus temperature space (Fig. 9).

Between 221 and 238 K, the RH at which depositional ice nucleation occurs on the hydrated particles increases from 62 to 79 % (S_{ice} = 1–1.11). Similarly, between 235 and 239 K, the RH at which deliquescence occurs increases from 77 to 93 %

ACPD
11, 23139–23167, 2011

(S_{ice} = 1.11–1.30). In this temperature region (denoted with the gray shading) both deliquescence and depositional ice nucleation occurs. As the temperature is warmed from 239 K, only deliquescence occurs and the DRH decreases. The shapes of the depositional ice nucleation and deliquescence curves show that the data are consistent with one another. At temperatures warmer than 239 K, the particles will deliquesce and at temperatures below 235 K the particles will depositionally nucleate ice.

4 Atmospheric implications

The results of this study show that the hydrated form of $NaCl_{(s)}$ is a very good IN. However, it is not known whether or not hydrated $NaCl_{(s)}$ is present enough of the time in the troposphere to affect ice nucleation. Therefore, the water uptake and depositional ice nucleation data collected in this study for $NaCl_{(s)}$ and hydrated $NaCl_{(s)}$ was used in a trajectory model following the approach used by Jensen et al. (2010). The result of the model is shown graphically in Fig. 10. Specifically, the temperature, relative humidity, and NaCl phase was tracked along parcel trajectories after they were detrained from deep convection (at 100% RH) (see Jensen et al., 2010 for details). It was calculated, at temperatures below 220 K, that hydrated $NaCl_{(s)}$ is present 40–80 % of the time in the troposphere.

Because hydrated $NaCl_{(s)}$ particles could be frequently present, they could play a role in cirrus cloud formation. Cziczo et al. (2004) found that sea salt was often incorporated in anvil cirrus clouds formed near the Florida peninsula. They hypothesized that the ice crystals formed via a homogeneous nucleation mechanism. However, the current study suggests that a different pathway of ice formation for the anvil cirrus clouds is possible. If the temperature and RH conditions are right, hydrated $NaCl_{(s)}$ can compete with mineral dust for ice nucleation via a heterogeneous mechanism.

In addition to impacting atmospheric ice, hydrated $NaCl_{(s)}$ may also have a climactic impact. The ratio of the radiative forcing, ΔF_R, of the hydrated NaCl particles (denoted with a subscript "h") with respect to the anhydrous particles (denoted with a subscript "dry") is calculated using the equation (Chylek and Wong, 1995)

ACPD
11, 23139–23167, 2011

$$\Delta F_{\mathrm{R}} = \frac{Q_{\mathrm{exp,h}} D_{\mathrm{h}} \left(1 - \frac{g_{\mathrm{h}}}{2}\right)}{Q_{\mathrm{exp,dry}} D_{\mathrm{dry}} \left(1 - \frac{g_{\mathrm{dry}}}{2}\right)} \quad (1)$$

where Q_{ext} is the extinction efficiency, D is the particle diameter and g is the asymmetry parameter.

The ratio of diameters for the hydrated to anhydrous NaCl was determined experimentally. The ratio of diameters is usually expressed as a growth factor, G_{f}.

$$G_{\mathrm{f}} = \frac{D_{\mathrm{h}}}{D_{\mathrm{dry}}} \quad (2)$$

Using the optical microscope, anhydrous particle diameters were first measured. Then particles were deliquesced and their sizes measured, followed by efflorescence at temperatures between 239 and 249 K. Efflorescence resulted in hydrated particles. The same particles were thus measured in the dry, deliquesced and hydrated state and growth factors on a particle by particle basis were determined. Using a population of 93 particles, an average growth factor of 2.01 ± 0.22 was measured for the deliquesced particles at an average RH of 81.6 %. Using a population of 52 particles, an average growth factor of 1.46 ± 0.13 was measured for the hydrated $NaCl_{(s)}$ particles. The value obtained for aqueous $NaCl_{(aq)}$ is in agreement with the prediction from the E-AIM model of 1.98 at 81.6% RH (Clegg et al., 1998, http://www.aim.env.uea.ac.uk/aim/aim.php). This gives us added confidence that the growth factor for the hydrated NaCl particles is a reasonable approximation.

To use Eq. (1) to determine the radiative forcing ratio, it is also necessary to estimate the extinction efficiencies and asymmetry parameters. Both of these values were calculated using MATLAB versions of Mie codes adapted from Bohren and Huffman (2004) and Mätzler (2002). As input into the Mie calculations, the refractive indices of the dry and hydrated NaCl are needed. The literature value for the real refractive indices at 589 nm of pure $NaCl_{(s)}$ and water are 1.54 and 1.33, respectively (CRC, 2011). The

ACPD
11, 23139–23167, 2011

refractive index of the hydrate was calculated in two ways. Using densities for the bulk compounds and the formula weight assuming a dihydrate, the molar volume was calculated. Using the refractive indices of the pure compounds, a volume-weighted refractive index ($n = 1.42$) was determined for the hydrate. The measured growth factor can also be used to estimate the volume of water relative to the NaCl. This results in a very similar refractive index for the hydrate of 1.40.

ΔF_R was calculated at 532 nm for hydrated relative to anhydrous NaCl for particles with diameters between 0.1 µm to 10 µm and the results are shown in Fig. 11. The oscillations observed in Fig. 11 are caused by the oscillations observed in Mie scattering curves as a function of size parameter. The positive value of ΔF_R observed over all sizes indicates an enhancement in cooling for the hydrates. The enhancement is largest for the smallest particle sizes. The average ΔF_R for particles 1 µm in diameter and larger is 2.0 for hydrated $NaCl_{(s)}$ relative to $NaCl_{(s)}$. Thus neglect of hydration for NaCl particles could lead to a factor of two error in the calculated radiative forcing.

5 Conclusions

In this manuscript we have presented new laboratory experiments showing the formation of a NaCl hydrate upon efflorescence of small NaCl droplets at low temperatures. This hydrate is a better ice nucleus than dry NaCl particles as it does not require any significant supersaturation at temperatures below about 235 K. Model calculations of the potential occurrence of the hydrated NaCl particles in the upper troposphere together with radiative transfer calculations suggest a significant impact on the radiative forcing of such particles.

Acknowledgements. The authors gratefully acknowledge the National Science Foundation for supporting this work (NSF-ATM 0650023 and AGS1048536). K. Baustian received additional support from NASA (NESSF fellowship NN08AU77H) and by CIRES at the University of Colorado at Boulder. T. K. acknowledges funding from European Commission (505390-GOCE-CT-2004).

ACPD
11, 23139–23167, 2011

References

CRC Handbook of Chemistry and Physics (Internet version 2011), 91 ed., edited by: Lide, D. R., CRC Press, Boca Raton, 2011.

Baustian, K. J., Wise, M. E., and Tolbert, M. A.: Depositional ice nucleation on solid ammonium sulfate and glutaric acid particles, Atmos. Chem. Phys., 10, 2307–2317, doi:10.5194/acp-10-2307-2010, 2010.

Biskos, G., Malinowski, A., Russell, L. M., Buseck, P. R., and Martin, S. T.: Nanosize effect on the deliquescence and the efflorescence of sodium chloride particles, Aerosol Sci. Technol., 40, 97–106, 2006.

Blanchard, D. C.: The oceanic production of atmospheric sea salt, J. Geophys. Res., 90, 961–963, 1985.

Bohren, C. F. H. and Huffman, D. R.: Absorption and scattering of light by small particles, Wiley-VCH, Weinheim, Germany, 2004.

Chylek, P. and Wong, J.: Effect of absorbing aerosols on global radiation budget, Geophys. Res. Lett., 22, 929–931, 1995.

Clegg, S. L., Brimblecombe, P., and Wexler, A. S.: A thermodynamic model of the system H^+-NH_4^+ -Na^+- SO_4^{2-}- NO^{3-} -Cl^-- H_2O at 298.15 K, J. Phys. Chem. A, 102, 2155–2171, 1998.

Cziczo, D. J. and Abbatt, J. P. D.: Infrared observations of the response of NaCl, $MgCl_2$, NH_4HSO_4, and NH_4NO_3 aerosols to changes in relative humidity from 298 to 238 K, J. Phys. Chem. A, 104, 2038–2047, 2000.

Cziczo, D. J., Murphy, D. M., Hudson, P. K., and Thomson, D. S.: Single particle measurements of the chemical composition of cirrus ice residue during CRYSTAL-FACE, J. Geophys. Res., 109(13), D04201, doi:10.1029/2003jd004032, 2004.

De Haan, D. O. and Finlayson-Pitts, B. J.: Knudsen cell studies of the reaction of gaseous nitric acid with synthetic sea salt at 298 K, J. Phys. Chem. A, 101, 9993–9999, 1997.

Dubessy, J., Audeoud, D., Wilkins, R., and Kosztolanyi, C.: The use of the Raman microprobe MOLE in the determination of the electrolytes dissolved in the aqueous phase of fluid inclusions, Chem. Geol., 37, 137–150, 1982.

Haywood, J. M., Ramaswamy, V., and Soden, B. J.: Tropospheric aerosol climate forcing in clear-sky satellite observations over the oceans, Science, 283, 1299–1303, 1999.

Jensen, E. J., Pfister, L., Bui, T.-P., Lawson, P., and Baumgardner, D.: Ice nucleation and cloud microphysical properties in tropical tropopause layer cirrus, Atmos. Chem. Phys., 10, 1369–1384, doi:10.5194/acp-10-1369-2010, 2010.

ACPD
11, 23139–23167, 2011

Koop, T.: Homogeneous ice nucleation in water and aqueous solutions, Z. Phys. Chem., 218, 1231–1258, 2004.
Koop, T., Kapilashrami, A., Molina, L. T., and Molina, M. J.: Phase transitions of sea-salt/water mixtures at low temperatures: Implications for ozone chemistry in the polar marine boundary layer, J. Geophys. Res., 105, 26393–26402, 2000.
IAP Research Report, No. 2002-08: http://diogenes.iwt.uni-bremen.de/vt/laser/wriedt/Mie_Type_Codes/body_mie_type_codes.html (last access: May 2008), 2002.
Martin, S. T.: Phase transitions of aqueous atmospheric particles, Chem. Rev., 100, 3403–3453, 2000.
Middlebrook, A. M., Murphy, D. M., and Thomson, D. S.: Observations of organic material in individual marine particles at Cape Grim during the First Aerosol Characterization Experiment (ACE 1), J. Geophys. Res., 103, 16475–16483, 1998.
Mikhailov, E., Vlasenko, S., Martin, S. T., Koop, T., and Pöschl, U.: Amorphous and crystalline aerosol particles interacting with water vapor: conceptual framework and experimental evidence for restructuring, phase transitions and kinetic limitations, Atmos. Chem. Phys., 9, 9491–9522, doi:10.5194/acp-9-9491-2009, 2009.
Pilson, M. E. Q.: An Introduction to the Chemistry of the Sea, Prentice Hall, Upper Saddle River, NJ, 1998.
Solubilities of Inorganic and Metal Organic Compounds, 4th ed., edited by: Linke, W. F., American Chemical Society, Washington DC, 1965.
Tang, I. N., Munkelwitz, H. R., and Davis, J. G.: Aerosol growth studies – II. Preparation and growth measurements of monodisperse salt aerosols, J. Aerosol Sci., 8, 149–159, 1977.
Vinoj, V. and Satheesh, S. K.: Measurements of aerosol optical depth over Arabian Sea during summer monsoon season, Geophys. Res. Lett., 30, 1263, doi:10.1029/2002GL016664, 2003.
Wise, M. E., Biskos, G., Martin, S. T., Russell, L. M., and Buseck, P. R.: Phase transitions of single salt particles studied using a transmission electron microscope with an environmental cell, Aerosol Sci. Technol., 39, 849–856, 2005.
Wise, M. E., Martin, S. T., Russell, L. M., and Buseck, P. R.: Water uptake by NaCl particles prior to deliquescence and the phase rule, Aerosol Sci. Technol., 42, 281–294 2008.
Wise, M. E., Baustian, K. J., and Tolbert, M. A.: Internally mixed sulfate and organic particles as potential ice nuclei in the tropical tropopause region, P. Natl. Acad. Sci. USA, 107, 6693–6698, doi:10.1073/pnas.0913018107, 2010.

ACPD
11, 23139–23167, 2011

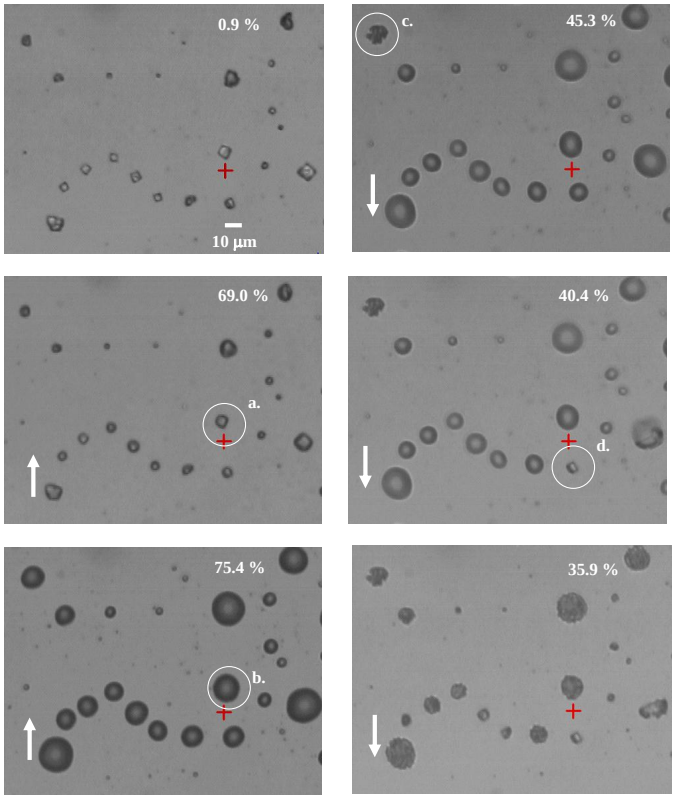

Fig. 1. NaCl particles at 244 K as RH is cycled. The up arrows indicate increasing water vapor in the environmental cell and the down arrows indicate decreasing water vapor in the environmental cell. The letters highlighting specific particles in this figure correspond to the letters denoting specific Raman spectra in Fig. 2. The cross in each panel corresponds to the point at which the Raman laser is positioned.

ACPD
11, 23139–23167, 2011

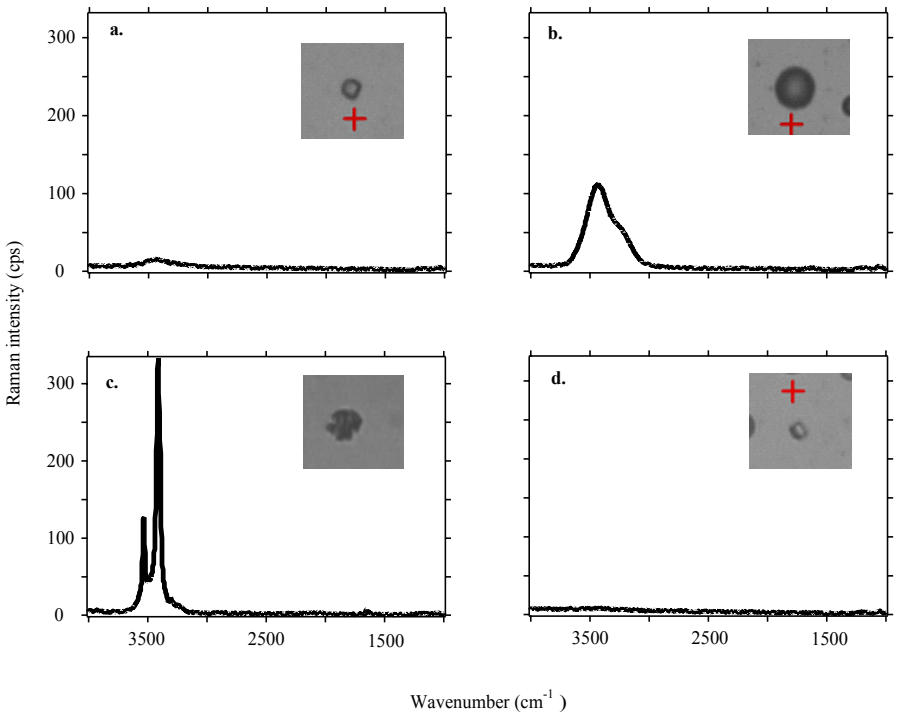

Fig. 2. Raman spectra of the particles highlighted in Fig. 1.

ACPD
11, 23139–23167, 2011

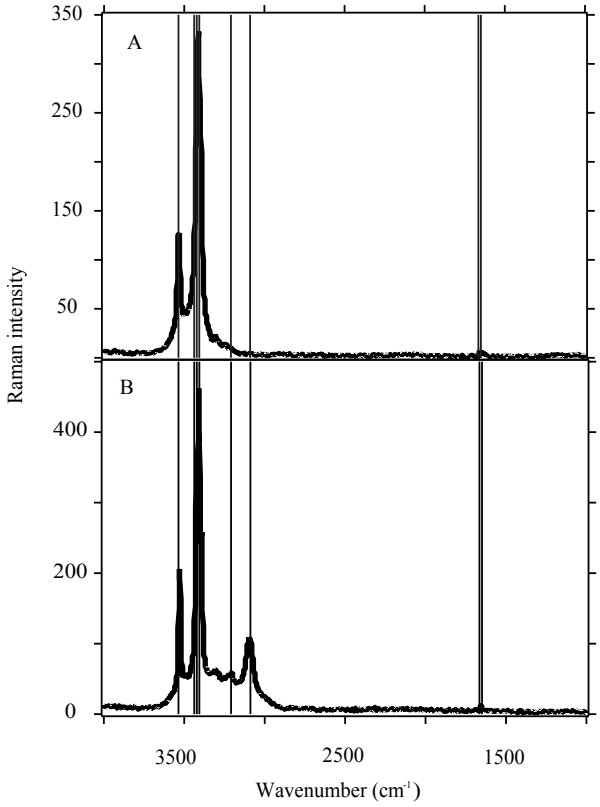

Fig. 3. (A) Raman spectrum of the non-cubic form of solid NaCl collected at 244 K. **(B)** Raman spectrum of the non-cubic form of solid NaCl collected at 163 K. The solid vertical lines highlight the peaks in Raman spectrum collected by Dubessy et al. (1982) for solid sodium chloride dihydrate.

ACPD
11, 23139–23167, 2011

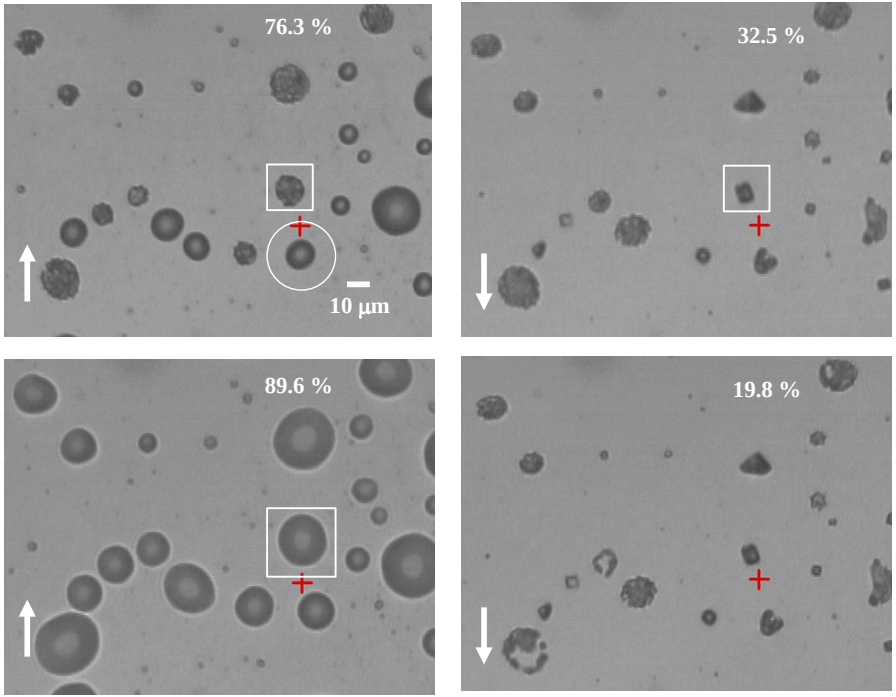

Fig. 4. NaCl particles (at 50× magnification) at 244 K as RH is cycled a second time. The up arrows indicate that water is being added to the environmental cell and the down arrows indicate that water is being removed from the environmental cell.

ACPD
11, 23139–23167, 2011

Depositional ice nucleation onto hydrated NaCl particles

M. E. Wise et al.

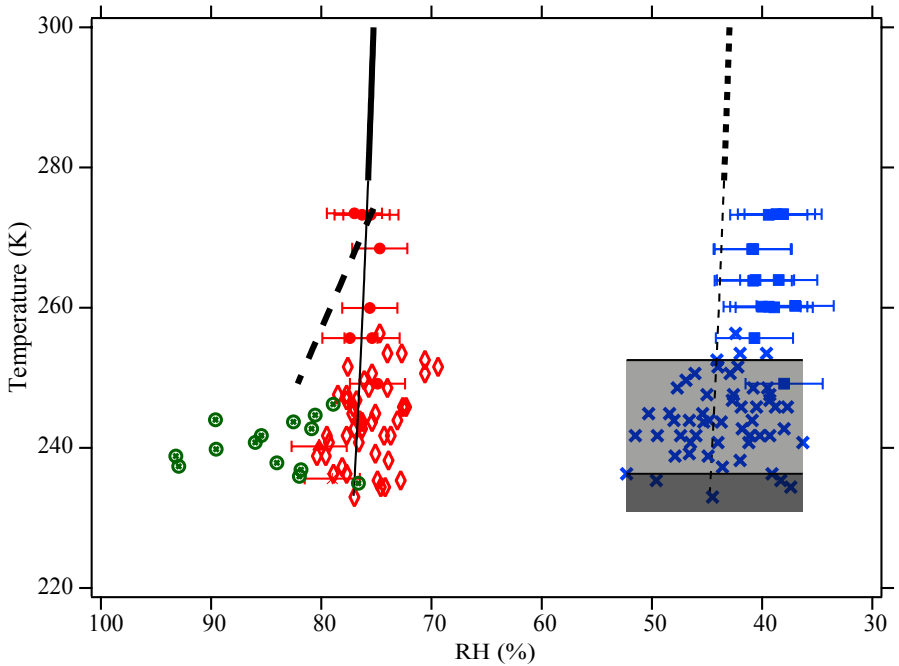

Fig. 5. NaCl phase diagram adapted from Koop et al. (2000): NaCl ERH (solid blue squares), NaCl DRH (solid red circles, triangle and star), accepted high temperature NaCl DRH (solid black vertical line), accepted high temperature NaCl ERH (dotted black vertical line), theoretical NaCl hydrate DRH (thick black dashed line). Data collected from Wise et al. (2011): NaCl hydrate DRH (crossed green circles), NaCl DRH (open red diamonds), NaCl ERH (blue crosses), region where mixed partcles effloresce (light gray shade), region where hydrated particles effloresce (dark gray shade).

ACPD
11, 23139–23167, 2011

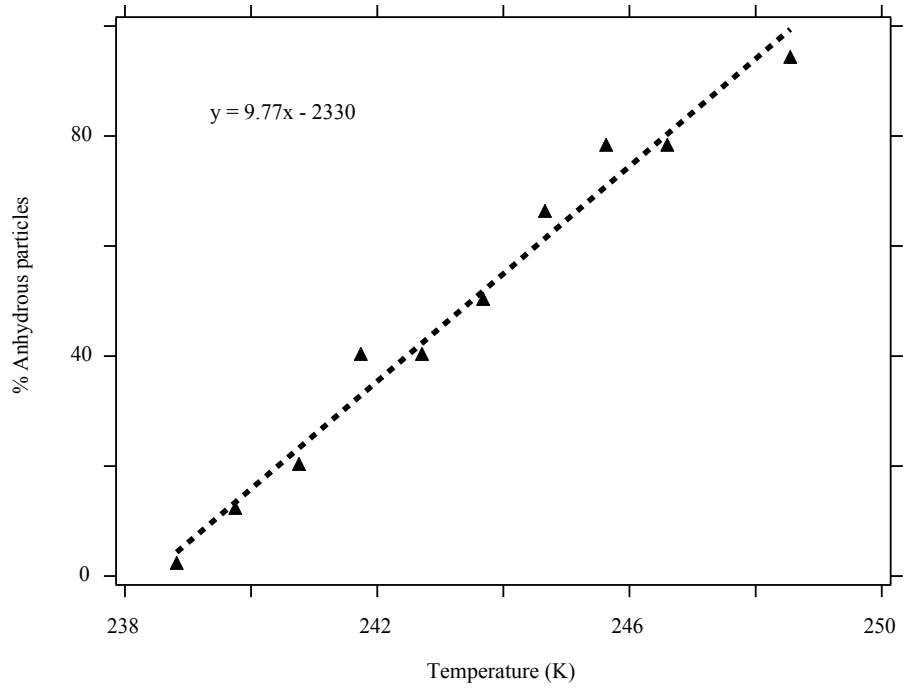

Fig. 6. Percent anhydrous particles versus temperature (K).

ACPD
11, 23139–23167, 2011

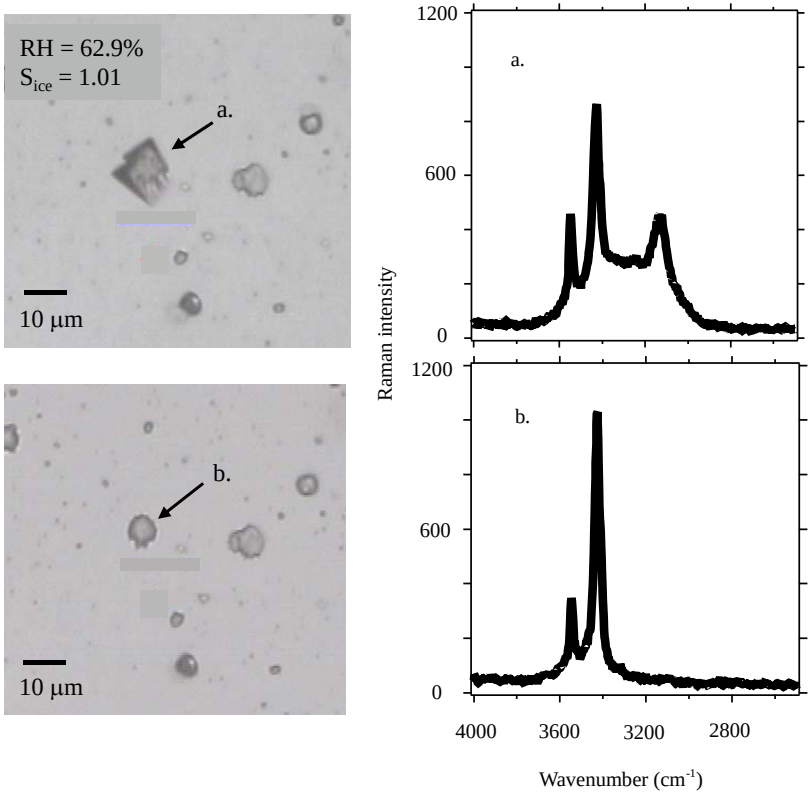

Fig. 7. Depositional ice nucleation experiment performed at 223 K on a mixed hydrated/anhydrous $NaCl_{(s)}$ sample. Particle "a" in the top left image is an ice particle which nucleated on a hydrated $NaCl_{(s)}$ particle at an Sice value of 1.01. Particle "b" in the lower left image is the ice nucleus after the ice was sublimed. Raman spectra of both particles were taken to confirm the presence of ice and the hydrated $NaCl_{(s)}$ particle.

ACPD
11, 23139–23167, 2011

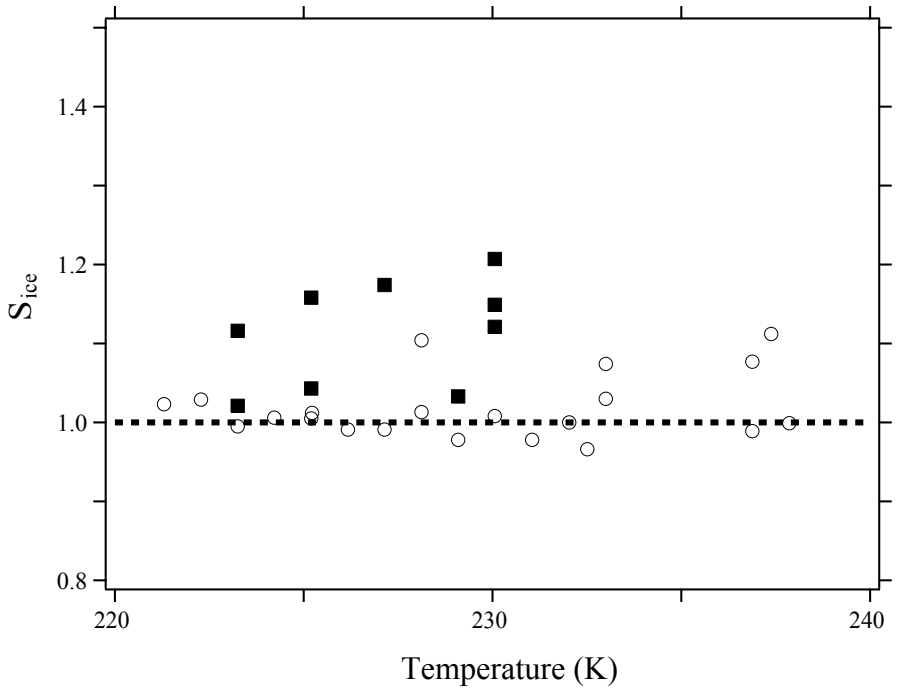

Fig. 8. S_{ice} versus temperature for depositional ice nucleation on NaCl (solid squares) and hydrated NaCl particles (open circles). An S_{ice} of 1 is denoted with the dotted.

ACPD
11, 23139–23167, 2011

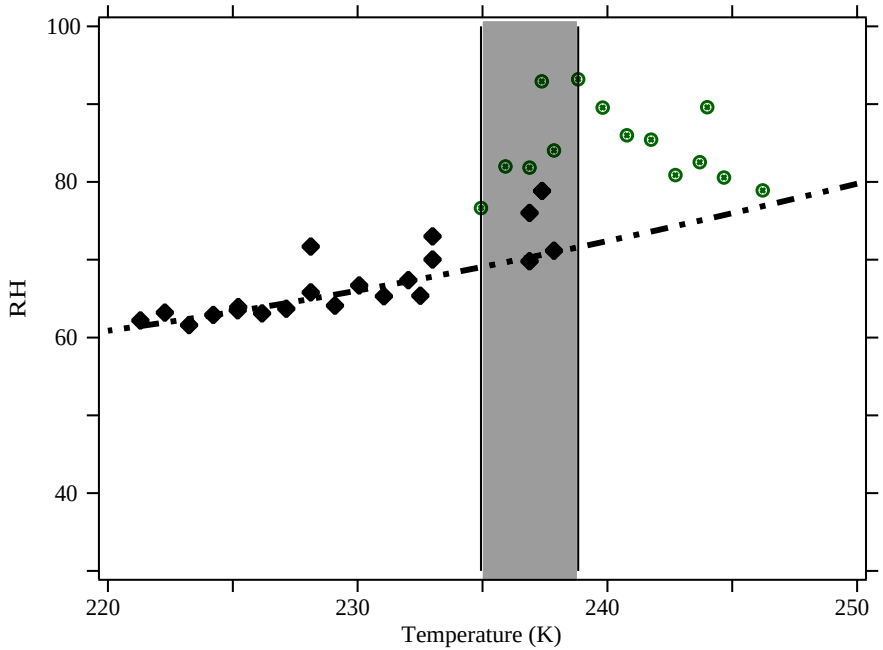

Fig. 9. Relative humidity versus temperature for depositional ice nucleation on hydrated $NaCl_{(s)}$ (filled diamonds) and deliquescence of hydrated $NaCl_{(s)}$ (crossed green circles). The grey shading denotes the temperatures at which both depositional ice nucleation and deliquescence occur. The dashed-dotted line represents RH at an $S_{ice} = 1$.

ACPD
11, 23139–23167, 2011

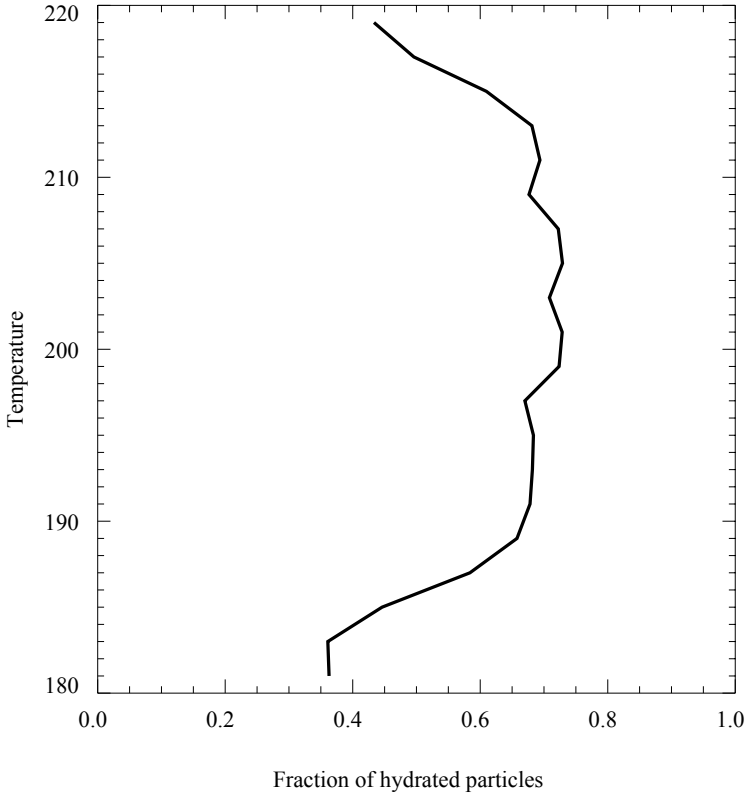

Fig. 10. Fraction of hydrated particles at temperatures ranging from 180 to 220 K.

ACPD
11, 23139–23167, 2011

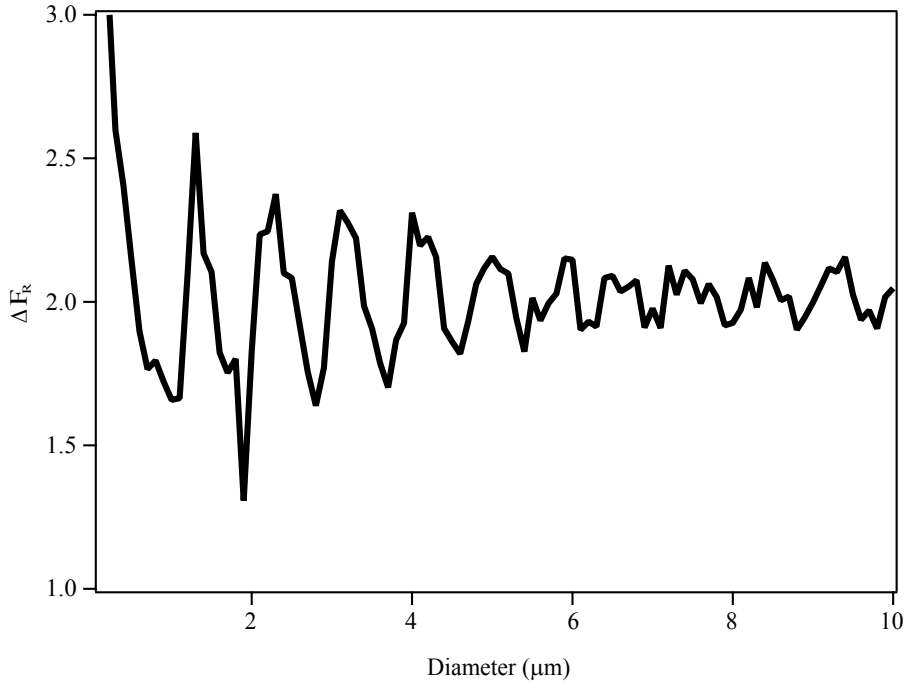

Fig. 11. Ratio of the radiative forcing of hydrated $NaCl_{(s)}$ particles with respect to dry particles (ΔF_R) as a function of particle diameter.

ACPD
11, 23139–23167, 2011